A Head-Up Display-Based P300 Brain–Computer Interface for Destination Selection

Luzheng Bi, Xin-An Fan, Nini Luo, Ke Jie, Yun Li, and Yili Liu

IEEE Transactions on Intelligent transportation systems (2013.12)

Presenter : Soogil Woo
GIST, Dept. of Information and Communication, INFONET Lab.

Gwangju Institute of Science and Technology

Introduction

- Brain–computer interfaces (BCIs) can translate user brain activity patterns into corresponding commands to communicate with or control the external world without using conventional communication channels.
- The brain signals widely used to develop EEG-based BCIs include:

➢ 1) P300 potentials, which are a positive potential deflection on the ongoing brain activity signal at latency of roughly 300 ms after the random occurrence of a desired target stimulus from nontarget stimuli

➢ 2) steady-state visual evoked potentials (SSVEPs), which are visually evoked by a stimulus modulated at a fixed frequency and occur as an increase in EEG activities at the stimulus frequency; and

➢ 3) the event-related desynchronizations (ERDs) and event-related synchronization (ERS), which are induced by performing mental tasks such as motor imagery, mental arithmetic, or mental rotation.

Introduction

- Since P300-based BCI systems are more suitable to output more commands compared with SSVEP-based and ERD/ERS-based BCI systems and have a relatively high level of accuracy, P300-based BCIs are currently used for destination selections.
- The preliminary experimental results provide an indication of the feasibility of using EEG to drive a vehicle.
- However, they did not describe the specific speed of the controlled simulated car and the specific accuracy.

Introduction

- Their long-term goal is to develop a brain-controlled vehicle by using BCI systems to select a destination and issue a control command.
- In this paper, they proposed a new P300 BCI with visual stimuli presented on a windshield via a head-up display (HUD) and develop a destination selection system for a simulated vehicle using the proposed BCI.
- Furthermore, to improve the usability of this destination selection system, they analyze the effects of the number of rounds of EEG on the performance of the proposed system.
- This paper lays a foundation for developing a brain-controlled vehicle that uses a BCI to select a desired destination from a list of predefined destinations and then uses an autonomous navigation system to reach the desired destination.

Head-up Display

- A HUD is any transparent display that presents data without requiring users to look away from their usual viewpoints.
- HUDs were initially developed for military aviation, they are now used in commercial aircraft, automobiles, and other applications.

Hud-Based P300 BCI for destination selection

A. Visual Stimuli

- The P300 visual stimuli used in this paper are a 3*3 matrix of characters, which are displayed on a real windshield (whose top, bottom, left, and right edges are 102, 138, 59, and 59 cm) of vehicles via a HUD system constructed by ourselves.

- Each character represents a predefined destination.

  "B" -> "Bank", "H" -> "Hospital."

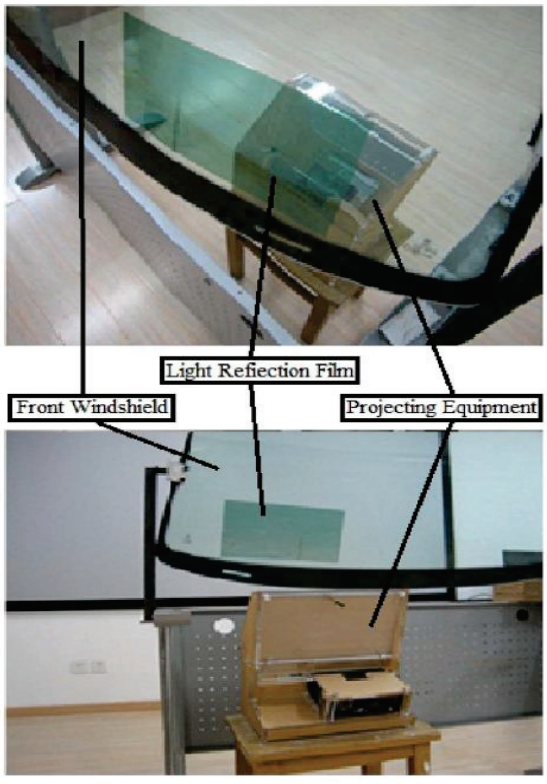

Fig. 1. HUD system.

Hud-Based P300 BCI for destination selection

A. Visual Stimuli

- The HUD system consists of a projecting device and some light reflection films (17.5 cm * 13 cm in size) pasted on the bottom-left area of the windshield.
- All of the nine characters flash on the windshield in sequence and in random order in each round.
- Each flash lasts 125 ms with an interstimulus interval of 15 ms, and thus, each round takes 1260 ms ((125 + 15) * 9).
- When the user wants to reach a destination, he focuses attention on the character associated with the destination, and the BCI interprets the EEG to infer the character to which the user is attending.

Hud-Based P300 BCI for destination selection

B. Data Collection

- They used a 16-channel amplifier to acquire the EEG signals at eight standard locations (i.e., Fz, Cz, Pz, Oz, P3, P4, P7, and P8), as shown in Fig. 2.
- The reference potential was the average of the potentials of the left and right earlobes.
- The EEG signals were amplified and digitalized with a sampling rate of 1000 Hz and a power-line notch filter to remove the line noise.

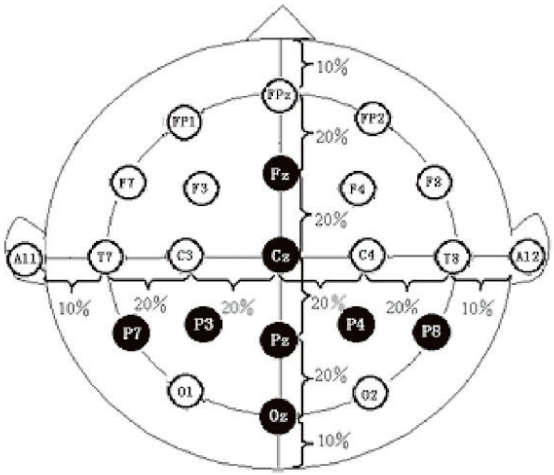

Fig. 2. Placements of eight channels used to collect EEG data are marked in black.

Hud-Based P300 BCI for destination selection

C. Signal Processing and Classification

- The collected EEG data are first decimated by a factor of 2 and filtered with a bandpass filter between 0.53 and 15 Hz.
- To improve the signal-to-noise ratio, *M* rounds of EEG data are summed. (M is number)
- To reduce the feature dimensionality in order to lower the redundancy of the features, the principal component analysis (PCA) is used, which transforms the feature space into an orthogonal space consisting of uncorrelated variables called principal components, and selects components with the highest eigenvalues as new features.

Hud-Based P300 BCI for destination selection

C. Signal Processing and Classification

- The input to the classifier of P300 is a vector of *N* dimensions, as follows:

$$x = [x(1), x(2), \ldots, x(N)]$$

➢ where *x*(*N*) is the *N*th new feature of each sample selected from the original features by using PCA.

- Linear discriminant analysis (LDA) was first used to develop the classifier, which can be represented in the following form

$$y = w^T x$$

➢ where *w* is the projection direction determined by maximizing the following cost function.

$$J_F(w) = \frac{w^T S_b w}{w^T S_w w}$$

➢ where S_b is the between-class scatter matrix, and S_w is the within-class scatter matrix.

Experiment

A. Experimental Platform

- A simulated vehicle has been designed and constructed. It includes three main parts, as shown in Fig. 3.
- 1) the HUD-based P300 BCI system for destination selection.
- 2) the 3-D driving scene and simulated vehicle based on the virtual reality technology.
- 3) the communication system between the computer supporting the 3-D driving scene and virtual vehicle.

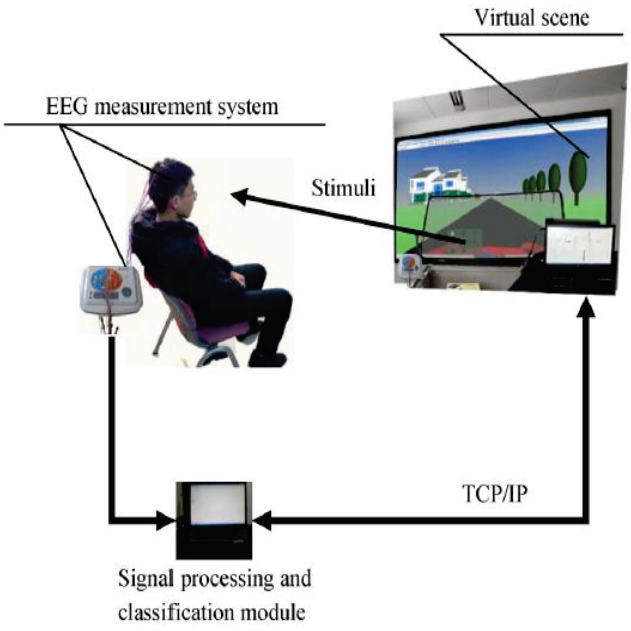

Fig. 3. Block diagram of the brain-controlled virtual vehicle.

Experiment

B. Experimental Procedures

- The experimental procedure includes two phases.
- The first is for training the HUD-based P300 BCI model for destination selection, and the second one is for evaluating and testing the destination selection system.
- In the phase of training the destination selection model, each participant completed four sessions of the P300 experiment in order to collect the data and train the model offline.
- In the second phase, they investigated the effects of the number of EEG rounds on the performance of the proposed system and demonstrated the simulated vehicles based on the destination selection system using a static and a dynamic experiment.

Result

- They used the 108 training samples collected in the experimental procedure to determine the parameters of the model of each subject, and 50 features selected by PCA are used for each model.
- In practice, first, it is desirable for the destination selection system to have high accuracy and short selection time.
- They investigated the destination selection accuracy as a function of the number of rounds when this system is used online.
- Second, given the required accuracy and selection time, it is desirable to reduce the time needed to build the corresponding model.
- They analyzed the selection accuracy as a function of the number of rounds used in building the model of each subject given the required selection time.

Result

A. Destination Selection Accuracy

- Fig. 4 shows the accuracy of the HUD-based BCI system used to select a destination as a function of the number of rounds of EEG used online by the model of the selection system.
- In this figure, the *x*-axis represents the number of rounds whereas the *y*-axis represents the accuracy gained if the BCI system selects a destination using only as many rounds as the *x*-axis.

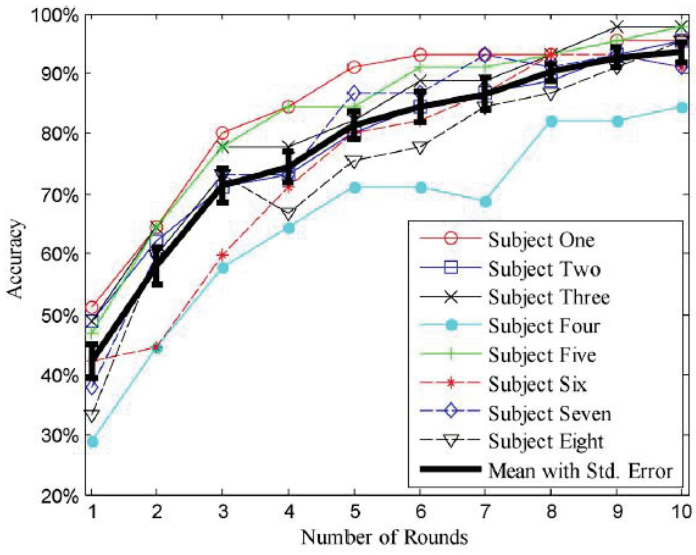

Fig. 4. Accuracy of the models as a function of the number of rounds of EEG data in testing.

Result

B. Reducing the Time Needed to Build a Model

- Given the desired accuracy and selection time to explore whether they can reduce the time needed to build the models, they analyzed the accuracy as a function of the number of rounds used in building the model of each subject.
- Fig. 5 shows the accuracy of the models as a function of the number of rounds used to build models by using ten rounds of EEG data to test each model.

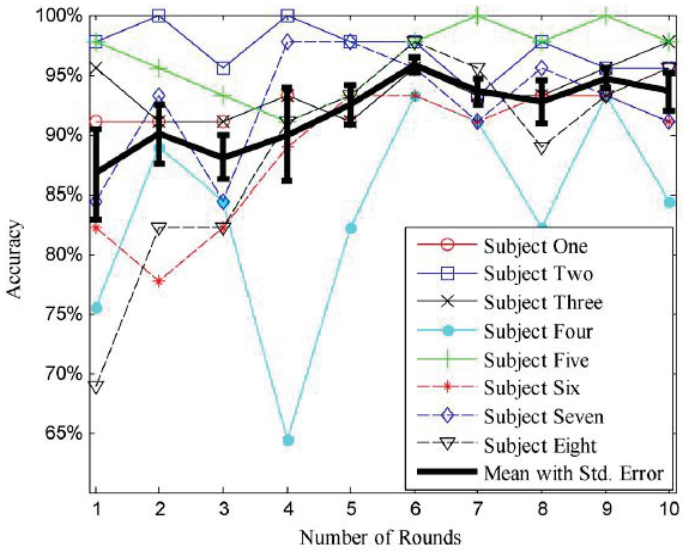

Fig. 5. Model accuracy as a function of the number of rounds of EEG data used in training the models.

Discussion and Conclusion

- First, although the accuracy is 93.6%, this accuracy may not be high enough for some applications.
- Second, the number of predefined destinations of the current system is small.
- Third, the users lose their control of the vehicle after the BCI-based destination selection system sends a destination to the autonomous vehicle.
- Fourth, they conducted the experiment in a laboratory, where the environmental factors were constant. However, in practice, vehicles are used outdoors.
- Their future work focuses on addressing the issues listed above and developing brain-controlled vehicles by combining the HUD-based BCI with other BCIs for issuing motion commands.
- The current and future research in this area will help further improve the mobility, independence, and quality of life for people with disabilities, as well as the general public.

Thank you!

Linear discriminant analysis (LDA)

- The LDA (also known as Fisher's LDA) approach aims to find the optimal direction, $\mathbf{w}_1$, to project data upon and maximize the Fisher ratio:

$$J(\mathbf{w}_1) = \frac{\mathbf{w}_1^T \mathbf{S}_\mathbf{B} \mathbf{w}_1}{\mathbf{w}_1^T \mathbf{S}_\mathbf{w} \mathbf{w}_1} \qquad \text{where, } \mathbf{S}_\mathbf{B} = (\mathbf{m}_1 - \mathbf{m}_2)(\mathbf{m}_1 - \mathbf{m}_2)^T$$
$$\mathbf{S}_\mathbf{w} = \sum_i (\mathbf{x} - \mathbf{m}_i)(\mathbf{x} - \mathbf{m}_i)^T$$

- The maximization of mean distances and minimization of class scatters.

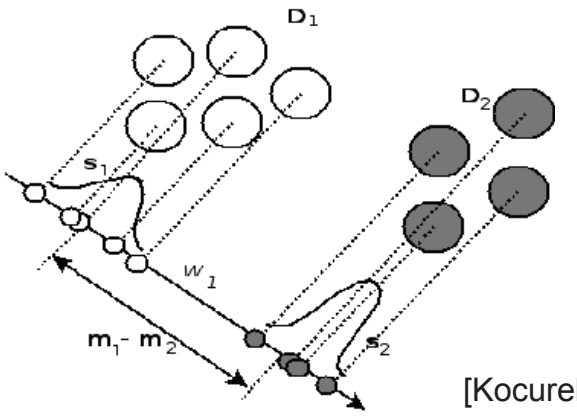

[Kocurek 2007]

Principal Component Analysis

- Eigen Vectors show the direction of axes of a fitted ellipsoid.
- Eigen Values show the significance of the corresponding axis.
- The larger the Eigen value, the more separation between mapped data.
- For high dimensional data, only few of Eigen values are significant.

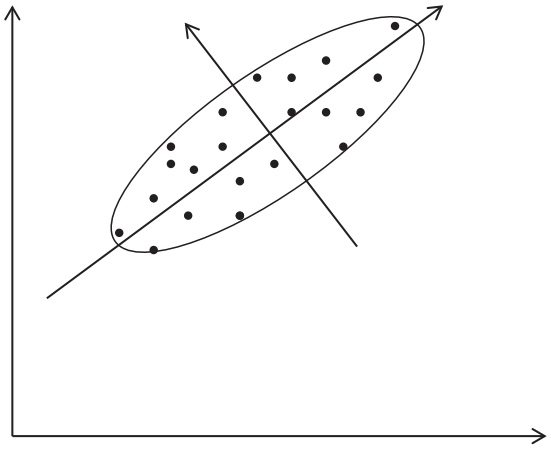

Title: Some fundamental properties of speckle.

Authors: J. W. Goodman.

Published in: J. Opt. Soc. Am., Vol. 66, No. 11, November 1976.

Presenter: Hwanchol Jang.

Abstract: A probabilistic modeling for speckle pattern is introduced. Ways to suppress the speckle pattern is also presented.

I. Introduction

Speckle

The vast majority of surfaces, synthetic or natural, are extremely rough on the scale of an optical wavelength. Under illumination by coherent light, the wave reflected from such a surface consists of contributions from many independent scattering areas. Interference of these de-phased but coherent wavelets results in the granular pattern we know as speckle.

Note that if the observation point is moved, the **path length**s traveled by the scattered components change, and a **new and independent valued of intensity** may results from the interference process.

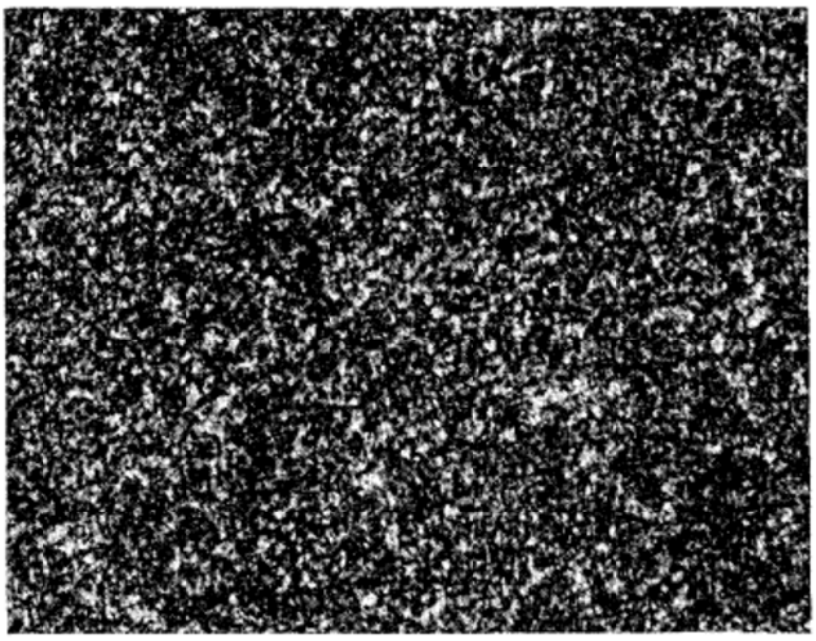

FIG. 1. Typical speckle pattern.

II. Speckle as a random-walk phenomenon

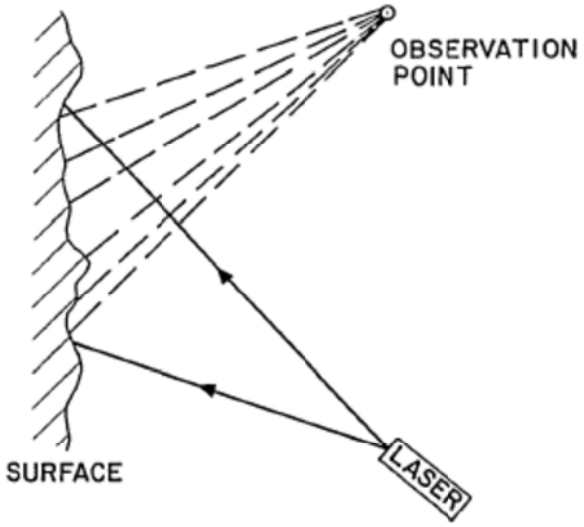

FIG. 2. Speckle formation in the free-space geometry.

The signal:

$$u(x, y, z; t) = A(x, y, z)\exp(i2\pi\nu t)$$

where ν is the optical frequency and $A(x, y, z)$ is a complex phasor amplitude

$$A(x, y, z) = A(x, y, z)\exp(i\theta(x, y, z)) .$$

The irradiance:

The directly observable quantity is the irradiance at (*x*,*y*,*z*), which is given by

$$I(x, y, z) = \lim_{T\to\infty}\int_{-T/2}^{T/2}\left|u(x, y, z; t)\right|^2 dt = \left|A(x, y, z)\right|^2 .$$

The complex amplitude of the field at (*x*,*y*,*z*) may be regarded as resulting from the sum of contributions from many elementary scattering areas on the rough surface. Thus the phasor amplitude of the field can be represented by

$$A(x,y,z)=\sum_{k=1}^{N}a_k=\sum_{k=1}^{N}|a_k|\exp(i\phi_k)$$

where $|a_k|$ and ϕ_k represent the amplitude and phase of the contribution form the *k*th scattering area and *N* is the total number of such contributions.

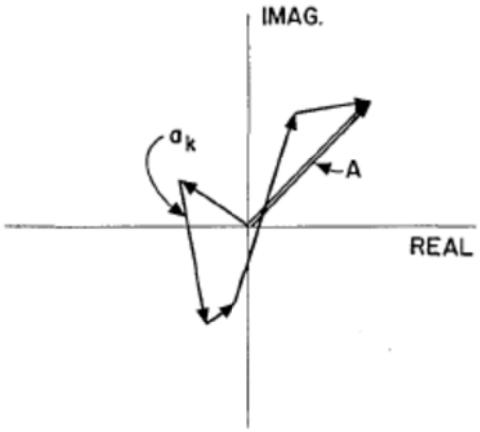

FIG. 4. Random walk in the complex plane.

Two important assumptions

(i) The amplitude and the phase of the *k*th elementary phasor are statistically independent of each other and of the amplitudes and phases of all other elementary phasors.

(ii) The phases of the elementary contributions are equally likely to like anywhere in the primary interval $(-\pi,\pi)$.

With these two assumptions, the similarity of our problem to the classical random walk in a plane becomes complete.

Provided the number *N* of elementary contributions is large, we find (a) the real and imaginary parts of the complex filed at (*x*,*y*,*z*) are independent, zero mean, identically distributed Gaussian random variables, and (b) the irradiance *I* obeys negative exponential statistics, i.e., its pdf is of the form

$$p(I)=\begin{cases}(1/\bar{I})\exp(-I/\bar{I}), & I\geq 0\\ 0, & \text{otherwise}\end{cases}$$

where $\bar{I}$ is the mean irradiance.

A fundamental important characteristic of the negative exponential distribution is that its standard deviation precisely equals its mean. Thus, the contrast of a polarized speckle pattern, as defined by

$$C = \sigma_I / \bar{I}$$

is always unity. Herein lies the reason for the subjective impression that the variations of irradiance in a typical speckle pattern are indeed a significant fraction of the mean.

III. Suppression of speckle

The sum of *M* identically distributed, real-valued, uncorrelated random variables has a mean value which is *M* times the mean of any one component, and a standard deviation which is $\sqrt{M}$ times the standard deviation of one component. Thus, if we add *M* uncorrelated speckle patterns on an irradiance basis, the contrast of the resultant speckle pattern is reduced in accord with the law

$$C = \sigma_I / \bar{I} = 1/\sqrt{M} \ .$$

Uncorrelated speckle patterns can be obtained from a given object by means of time, space, frequency, or polarization diversity.

Pure spatial diversity occurs, for example, when a reflecting surface is illuminated by several different lasers from different angles. If the **angles of illumination** are sufficiently separated, the path length delays experienced by each of the reflected beams will be different enough to generate uncorrelated speckle patterns.

A second way of changing optical paths (in wave lengths) traveled by a reflected wave is to change the optical **frequency of the illuminations**. If the separation of these frequency components is sufficiently great, *M* uncorrelated speckle patterns will result, with addition on an irradiance basis.

Ex) In a reflection geometry, with angles of incidence and reflection near normal to the surface, the separation required to produce uncorrelated speckle is approximately

$$\Delta \nu \cong c / 2\sigma_z$$

where c is the light velocity and σ_z is the standard deviation of the surface height fluctuations.

Time diversity: If a transparency object is illuminated through a diffuser, then motion of that diffuser results in a continuous changing of the speckle pattern in the image. A **time exposure** in the image plane then results in the addition, on an intensity basis, of a number of uncorrelated speckle patterns, thus suppressing the contrast of the detected speckle pattern.

IV. Discussion

The speckle phenomenon happens in turbid lens imaging (TLI) systems []. On the one hand, it is used as useful information. On the other hand, it is regarded as a noise that we try to suppress.

TLI is one new technique that increases the resolution of an imaging system beyond the physical limitation given by lenses. In TLI, a turbid medium is inserted between a sample and an objective lens. The turbid medium has many small particles in it, and the wavelets in the sample beam experience multiple scattering inside the medium. This scattering is good in a sense that higher angle mode waves, which usually go out of the detector, experience the scattering and may be redirected into the detector. This makes it possible to collect higher mode wave information which tells us the details of the sample. Also, the scattering is bad in a sense that it scrambles the sample image in the detector. But if we know i) the way how the medium scrambles images and ii) the way how to recover it using “i)”, it is no longer a problem. Here we can obtain “i)” because the input and output relationship of the turbid medium can be measured. “ii)” is also known as it is just an inverse problem given linear system model and the system response.

The sample beam is a weighted sum of waves with many spatial frequencies, written as follows,

$$x(t) = \sum_l x_l \exp(i2\pi f_l t)$$

where f_l is a spatial frequency and t is a spatial index.

We measure response of the optical system for a wave $\exp(i2\pi f_l t)$

$$T_l(t) = T\left(\exp(i2\pi f_l t)\right).$$

Assuming TLI system is linear time-invariant (LTI), the response to the input x can be written

$$y(t) = T(x(t)) = T\left(\sum_l x_l \exp(i2\pi f_l t) \right) = x_l \sum_l T_l \ .$$

Here, the index *t* and *l* actually have dimension two. Then, the response can be represented by a linear system model as follows

$$\mathbf{y} = \mathbf{T}\mathbf{x} \, .$$

Here, we can estimate **x** with given **y** and **T**, where **y** and **T** are measured in the experiments. Here, note that a column of **T** is a speckle pattern and the columns in **T** are uncorrelated to each other for their path lengths differ enough; if the spatial frequency gap is more than a certain value, it is true. So, we can see that the matrix **T** is well conditioned for recovery.

We also note that the **y** is in fact is a noisy measurement where speckle pattern is included in the noise. For the suppression of the noise, we can use multiple uncorrelated measurement as it is presented in the talk.